Proceedings of ASME 2016 International Mechanical Engineering Congress and Exposition
IMECE 2016
November 11-17, 2016, Phoenix, Arizona, USA

IMECE2016-67136

ABRASIVE WATERJET PROFILE CUTTING OF THICK TITANIUM/GRAPHITE FIBER METAL LAMINATE

Rishi Pahuja*
Department of Mechanical Engineering
University of Washington
Seattle, Washington 98195
rpahuja@uw.edu

M. Ramulu
Department of Mechanical Engineering
University of Washington
Seattle, Washington 98195
ramulum@u.washington.edu

M. Hahish
Flow International
Kent, Washington 98032
mhashish@flowcorp.com

ABSTRACT

Fiber Metal Laminates (FML) are one of the most advanced engineered materials used in aerospace industry. The combination of metallic sheets interspersed in composite laminates in one hybrid material system provides higher impact and corrosion resistance when compared with their monolithic counterparts. However, due to the difference in machining responses for different material phases, conventional machining often induce damages and defects, affecting the cost and structural performance of the part. This research study investigates the machinability of thermoplastic Titanium Graphite (TiGr) FML. The feasibility and machinability of contouring thick (7.6 mm−10.5 mm) TiGr through Abrasive Waterjet (AWJ) process was studied in terms of machined kerf characteristics- taper ratio and surface quality. The effect of a wide range of process parameters was investigated such as geometric variables (mixing tube aspect ratio and orifice bore size), kinetic variables (water pressure, jet traverse speed) and abrasive load ratio on the machining quality. Predictive mathematical regression models were developed through Analysis of Variance (ANOVA) in order to optimize the process. Alongside, machined surface was examined to inspect the topological characteristics, material removal mechanism, and machining induced damage (micro-defects) and distortion through Surface Profilometry, Scanning electron and optical microscopy. A comparison was drawn between conventional and AWJ trimming of TiGr to demonstrate the superiority and high speed machining of AWJ with less damage.

NOMENCLATURE

d_{entry}	Entry kerf width
d_{exit}	Exit kerf width
T	Specimen thickness
P	Pump Pressure
Lm/lm	Mixing tube length
dm	Mixing tube diameter
dn	Orifice diameter
R	Load ratio
u	Jet traverse speed
R_a	Average surface roughness
R_z	Ten-point average roughness

INTRODUCTION

The past few decades have witnessed significant focus in energy efficient systems which has seen no less than a global phenomenon. Material innovation, hitherto disregarded as a direct contributing factor to emission reduction and energy consumption, is gradually becoming the crux, especially for the heavy transportation sector. As a part of the development of high performance material, Fiber metal laminate (FML) is proven to be an important engineered material system, as evident from its widespread applications in aerospace and other industries where specific strength and modulus becomes a key driving factor. The next stage for this innovative material will be to serve in critical sections of aircrafts that could experience high skin temperatures (177 °C) due to aero-frictional heating at supersonic speeds. Titanium graphite (TiGr) is one of the primary candi-

*Address all correspondence to this author.

dates. It is composed of thin metal foils interspersed between composite laminates in a particular stacking sequence. The directional properties of composites with added benefits by metal foils such as protection of composite core from heat and moisture, better distribution of point load and enhanced compression after impact (CAI) strength renders high performance characteristics. These include high strength and stiffness to weight ratio and superior corrosion resistance, impact resistance, fracture resistance and better fatigue properties which helps to outperform either of the two constituent materials, making them superior to other conventional material systems [1–3].

Although TiGr laminates are molded/autoclaved to a near net shape, secondary processing such as drilling, peripheral machining and contouring to meet dimensional tolerances is often unavoidable. Traditionally, conventional machining processes have been employed for polymer matrix composites. However, machining becomes challenging owing to the inherent heterogeneity and anisotropy of composite materials. The abrasive nature of fibers leading to fiber pull-outs and debonding, delamination, thermal distortion, carcinogenic dust particles and high tool wear elevate the traditional machining cost [3, 4]. Besides, machining of titanium is challenging due to high strength, low stiffness and low thermal conductivity [5]. As apparent, machining of fiber metal laminates not only involves challenges to overcome the limitations posed by individual constituents, but also to ascertain a single process window to accommodate the difference in removal mechanism for all the three different phases viz. thermoplastic matrix, brittle fibers and ductile titanium. The most viable alternative is to adapt those unconventional processes where the machining response is less sensitive to the heterogeneity of the material system.

Several non-traditional methods have been explored for machining fiber metal laminates. Abrasive Waterjet is a widely used unconventional alternative because of superior process characteristics such as zero thermal damage in the workpiece, high cutting speed, wide working range and environmental friendly [6–8]. Although AWJ machining is promising for most of the material and shape feature applications, the process response variations due to continual energy loss throughout the penetration depth limits the maximum achievable thickness, which is a characteristic of almost all energy beam based machining processes. As established from previous investigations on AWJ machining of composites and ductile metals, process performance and associated cutting quality is significantly dependent on the type of workpiece material being machined due to difference in jet interaction and cutting mechanisms for different materials [7, 9, 10].

Several studies have been conducted for AWJ machining of titanium and CFRP individually [11–14]. Shipway et al. [11] and Ramulu et al. [12, 13] studied the abrasive waterjet machining of titanium alloys and identified several damages and challenges such as grit embedment and low traverse rate in comparison to aluminum, and ductile shearing, abrasive scooping and scratching action of abrasives as removal mechanisms respectively. Arola et al. [14] investigated the material removal mechanism in AWJ machining of unidirectional graphite/epoxy composite with 0°, 45° and 90° fiber orientation with reference to the cutting direction. They observed abrasive wear tracks near top kerf and high delamination at jet exit side along with extensive fiber pull-out. Several other research groups studied the machinability of polymer fiber composites through AWJ [15, 16]. It is apparent that machining of dissimilar material system is challenging due to possible machining variations introduced by completely different and ductile metal foils interspersed in composite plies with highly brittle fibers. Besides, the jet energy variation is accountable for low control and variable quality at different profile features (size and angles) within a contour geometry.

AWJ machining of fiber metal laminates is recently reported with material removal process and effect of operating parameters on AWJ machining of Glass fiber-Aluminum laminates [17]. However, the work is limited to machining of thin laminates ($\leq$ 2.5mm). Machining of TiGr is different from Glass/Aluminum laminates due to the presence of difficult-to-cut Titanium. Alberdi et al. [18] studied the machinability of CFRP/Ti6Al4V stacks for drilling operations and identified the processing window with high pressure and low feed rates to minimize taper angle and roughness. No detailed investigation on AWJ contouring and profile cutting of thick Titanium/graphite laminates has been reported to date. An evident need exists for a systematic AWJ machining evaluation and characterization of thick TiGr laminates, especially with thermoplastic matrix composite.

This research work is an extension of the preliminary study conducted on contouring thick TiGr laminates [19]. The study aims at quantification of the effects of a wide range of process parameters on surface quality and kerf taper ratio, identification of influential parameters and development of predictive mathematical models to facilitate parametric optimization. The effect of cutting geometry on the machining response is investigated and AWJ process is characterized for the machinability of thick TiGr FML. In addition, a comparison is drawn between AWJ and conventionally trimmed TiGr to foreground the limitations of conventional machining.

EXPERIMENT

Workpiece

Two 29.5 x 14.5 mm TiGr plates were obtained from an aerospace company, with two different thickness 10.50 mm and 7.56 mm. These plates were composed of graphite reinforced thermoplastic (PEEK) matrix composite layers and titanium alloy foils stacked together with autoclave consolidation process under different configuration for different thickness, as mentioned in Table 1. Both the laminates are spatially dominated by composites. The overall volumetric percentage of composite and titanium alloy is about 72% and 28% respectively in 7.56

TABLE 1. PLY THICKNESS AND LAYUP OF SPECIMENS.

Specimen Thickness (mm)	Ply Type and Ply Thickness (μm)		Number of Plies	Layup
10.75	Ti alloy	140	24	[0/-45/45/Ti/0/Ti/-45/45/Ti/0/Ti/-45/Ti/45/Ti/(0/Ti/45/Ti/45/Ti/0/Ti/-45/Ti/45/Ti/0/-45/Ti/45/-45/Ti/0)$_S$/45/Ti/-45/Ti/0]
	0° ply	210	12	
	45° ply	210	10	
	-45° ply	210	12	
7.56	Ti alloy	140	15	[(45/0/-45/45/0/-45/Ti/0/Ti/45/Ti/-45/Ti/45/Ti,0/Ti/-45/Ti/45)/Ti]$_S$
	0° ply	210	8	
	45° ply	210	10	
	-45° ply	210	8	

TABLE 2. PROPERTIES OF CONSTITUENT MATERIALS.

Material	Properties
Titanium alloy	33.75 GPa (Shear modulus),
(Ti-15V-3Cr-3Al-3Sn)	875 MPa (Shear strength)
Graphite/PEEK	8.9 GPa (Transverse modulus),
	80 MPa (Transverse strength)

mm thick laminate, and 68% and 32% in 10.5 mm thick laminate. The reason for selecting different layups for different levels of thickness is to facilitate capturing of the possible variations in AWJ machining behavior caused by the difference in ply arrangement, and to enable the study of machining characteristics of the laminates under a global qualitative function. The common properties of the constituent materials of as-obtained specimens are mentioned in Table 2.

Cutting Profile

Figure 1 illustrates the cutting profile geometry. The rationale behind selecting this geometry is to accommodate a wide range of cutting curvatures for intricate profiling applications in aerospace industry and possible replacement of drilling operation with trepanning [20]. Three levels of curved profiles, two characterized as small and one as large arc, are used in the cutting profile to study the effect of curvatures on machining responses. The curvature was varied between 0.04 and 0.1 mm^{-1} with total jet trajectory distance (projected linear length) of 216.18 mm, as mentioned in Table 3.

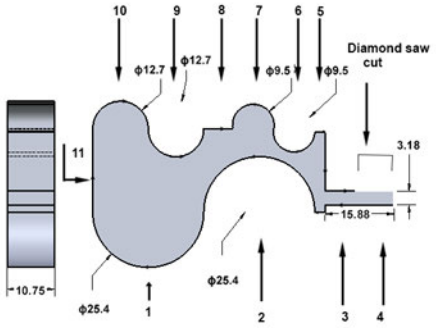

FIGURE 1. 2D CONTOUR PROFILE FOR AWJ MACHINING.

Experimental Design and Methodology

As shown in Fig. 2, Flow International® Waterjet facility equipped with 600 MPa Ultra high pressure intensifier was used. The experimental conditions and process variables with associated levels are given in Table 4. The geometric variables include orifice diameter, mixing tube length and diameter. Besides, the pump pressure, abrasive flow rate and jet traverse speed were varied for two thickness levels according to industrial judgement, previous investigations [10, 13, 17, 21] and pre-screening tests.

Orifice diameter to mixing tube diameter ratio was varied between 0.23 and 0.50. Mixing tube aspect ratio (length/diameter) was varied between 66.7 and 150. The standoff distance was maintained at 0.75 mm to ensure minimum energy loss before the jet interacts with workpiece and also to avoid pull-up delamination of top plies. Experimental design was obtained using optimal response surface design in Design-Expert v9.0.4 software. With 7 numeric factors, 192 experimental runs were obtained which were further reduced to 32 based on practical constraints. Table 5 in Appendix contains the design of experiments which is used to refer experimental conditions, hereinafter AWJ-X, 'X' being the corresponding experimental condition in Table 5.

Kerf ratio is defined as the ratio of jet entry kerf width and jet exit kerf width (Eqn. (1))

$$Kerf\ Taper\ Ratio = \frac{d_{entry}}{d_{exit}} \tag{1}$$

Top and bottom kerf width was measured using MicroVu Sol Precision measuring machine equipped with Programmable LED coax light and autofocus detection through 6.5X zoom lens. The kerf width was averaged for five different locations at each profile feature. The kerf surface profile was measured longitudinally (parallel to jet traverse direction) and transversely (orthogonal to jet traverse direction) on the machined surface. The surface roughness of the kerf wall was evaluated in terms of stan-

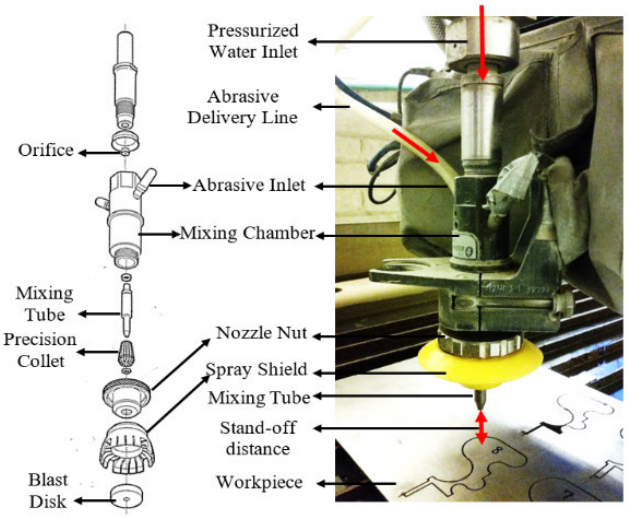

FIGURE 2. EXPERIMENTAL SETUP - NOZZLE ASSEMBLY.

TABLE 3. CUTTING PROFILE FEATURE DIMENSIONS.

Profile Number	Profile	Dimension (mm)	Projected linear length
1	Large outer arc	25.4	39.9
2	Large inner arc	25.4	39.9
(3, 4), 5, 8	Straight cut	15.88, 1.59, 6.35	15.88, 1.59, 6.35
7, 10	Small outer arc	9.6, 12.7	14.9, 19.95
6, 9	Small inner arc	9.6, 12.7	14.9, 19.95

dard roughness parameters using MarSurf XR 20 surface roughness measuring equipment. This XR 20 contact type profilometer was equipped with a stylus based, 2.5μm radius conical diamond tip with 5nm resolution. To inspect the machined surface integrity, selected specimens were sectioned using Buehler Isomet low speed saw with a diamond cutting wheel. The straight cut specimens were examined under Scanning Electron microscope.

In order to compare the AWJ machininig with conventional milling/trimming of TiGr, the 7.6 mm thick TiGr specimen was machined with a 4 flute, PVD coated cemented carbide end mill tool of cutting diameter 6.35 mm. Five different feed levels - 50.8, 152.4, 254, 381, 635 mm/min were used to produce five through cuts at 6000 rpm. The topological features were studied using SEM micrographs.

TABLE 4. Experimental conditions

Parameter	Description
Grit type	Garnet
Grit size (mesh)	120
Impact angle	90
Stand-off distance (mm)	0.75
Variable	Range
Nozzle (mm)	Length 76.2, 50.8 mm,
	Diameter: 0.508, 0.762 mm
Orifice (mm)	Sapphire,
	Diameter: 0.178, 0.254 mm
Specimen thickness (mm)	7.56, 10.50
Jet Pressure (MPa)	380, 600
Load ratio (%)	8.0, 9.2, 10.1
Jet traverse speed (mm/min)	50.8, 152.4

RESULTS AND DISCUSSION

Contrary to the understanding of machining composite laminates or monolithic titanium, a combination of these two materials (FMLs) raised some new concerns vis-à-vis kerf wall quality. The machining quality, assessed by variation of kerf width and surface profilometry, was helpful in outlining the effect of process parameters, as discussed in this section.

Kerf Taper Ratio

The taper ratio observed within the experimental range was 0.99-1.31 and 1.04-1.39 for 7.56 mm and 10.5 mm thick specimens respectively. Figure 3 shows the maximum and minimum kerf wall geometry for 7.56 mm and 10.5 mm thick specimens respectively. The figures depict maximum kerf angle variation and thus maximum damage location at the jet entry side where most of the plies are composite laminates. In general, thinner laminate showed a tendency of slightly curved kerf wall with convexity on both the kerf walls. This can be attributed to higher composite damage at the exit and entry side in thinner laminate whereas in thick laminate the composite composition is lesser at the entry and exit side, leading up to less damage at the extreme ends.

A response surface model, reduced to two factor interaction, was obtained with traverse speed and mixing tube geometry as the major contributing parameters. Some of the interaction terms were observed to be dominant in taper model. Figure 4 shows the

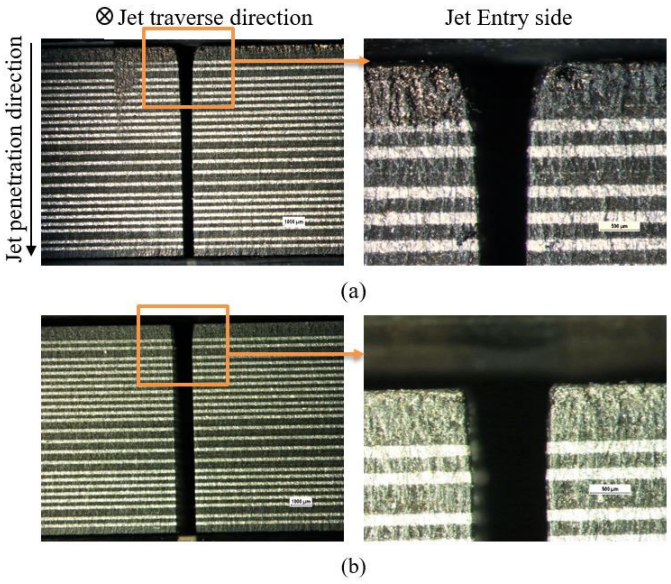

FIGURE 3. (a) MAXIMUM, AND (b) MINIMUM STRAIGHT CUT TAPER KERF WALL ASSOCIATED WITH EXPERIMENT CONDITIONS 32 AND 28 RESPECTIVELY.

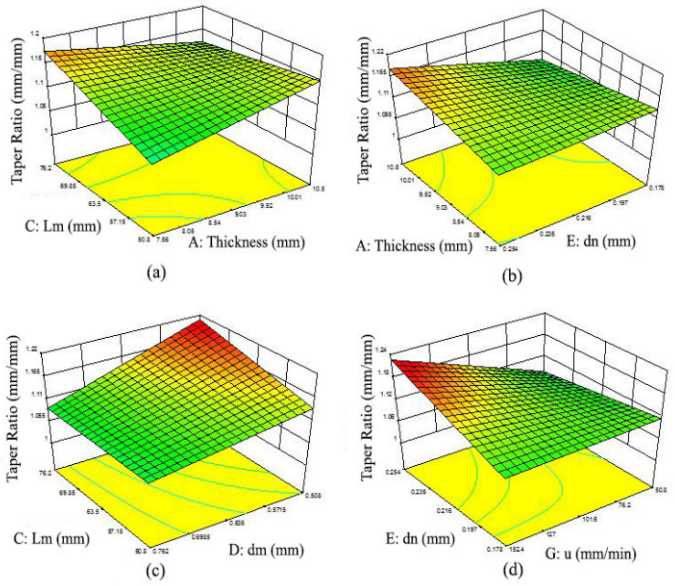

FIGURE 4. INTERACTION EFFECT BETWEEN (a) THICKNESS AND MIXING TUBE LENGTH, (b) THICKNESS AND ORIFICE DIAMETER, (c) MIXING TUBE LENGTH AND DIAMETER, AND (C) TRAVERSE SPEED AND ORIFICE DIAMETER ON KERF TAPER RATIO.

parametric effects on taper ratio, with non-variables fixed at their average values in each plot. As observed in Fig. 4(a), the kerf taper ratio was found to exhibit a negative trend with increasing mixing tube length for thicker specimens and vice versa for thinner specimens. The model predicted 2.31% reduction in taper ratio with 50% increment in mixing tube length from 50.8 mm to 76.2 mm for 10.5 mm thick specimens. However, for 7.56 mm thick specimens, kerf taper ratio exhibited positive trend with 8.19% increment in taper ratio as the mixing tube length was increased. Overall, this interaction effect can be interpreted as a desirability of higher mixing tube length at higher thickness in order to supplement the higher energy requirement due to increased cutting depth. A longer mixing tube would allow more time for energy transfer from water to abrasive particles and hence producing a more coherent and cutting efficient waterjet slurry. Similarly, a shorter mixing tube is expected to produce a low energy jet, leading up to a high taper ratio. However, it can be argued that a short mixing tube is sufficient to meet the less energy requirement of thinner specimens. This is supported by ANOVA results which show the use of mixing tube longer than the optimum would mean producing an abrasive jet with energy level higher than the required, creating more distortion and significantly high taper ratio, indicating the increased entry damage at prolonged exposure of the high energy jet. The results are coeval with the study conducted by Jegaraj et al. [22], emphasizing the existence of an optimum mixing tube at which the momentum transfer is maximum. Figure 4(b) shows the interaction effect between specimen thickness and orifice bore size on straight cut taper ratio. A negligible, but negative trend of taper ratio was observed with orifice bore size at lower thickness level (7.56 mm) while 8.12% increment in taper ratio was observed at higher thickness level (10.5 mm). The results were inconsistent with the established reasoning of increased water flow rate with orifice diameter at a given load ratio, thus increased abrasive flow rate and more cutting power, leading to less kerf taper. However, it can be argued that unlike metals, the mechanism of material removal in composites is significantly affected by the water power of the jet. It is evident from the results that a thicker laminate would have more effect of water power assisted by slow penetration and removal of composite plies, especially when the face sheets are composite plies, suggesting more distortion at the top and resulting in high taper ratio. Figure 4(c) depicts the interaction between mixing tube geometrical features- length and diameter on taper ratio. 4.8% and 9.8% increment in taper ratio with 33.3% reduction in mixing tube diameter was observed at mixing tube lengths 50.8 and 76.2 mm respectively. Overall, higher taper was observed at high aspect ratio (length/diameter) and least at low aspect ratio. With low orifice diameter and thus low mass flow rate of water as well as abrasives at a given load ratio, an insignificant variation of taper ratio with the traverse speed (-0.52%) was observed. However, the effect of traverse speed was dominating at large orifice diameter with a 14.22% decrease in taper ratio within the experimental limits of traverse speed lev-

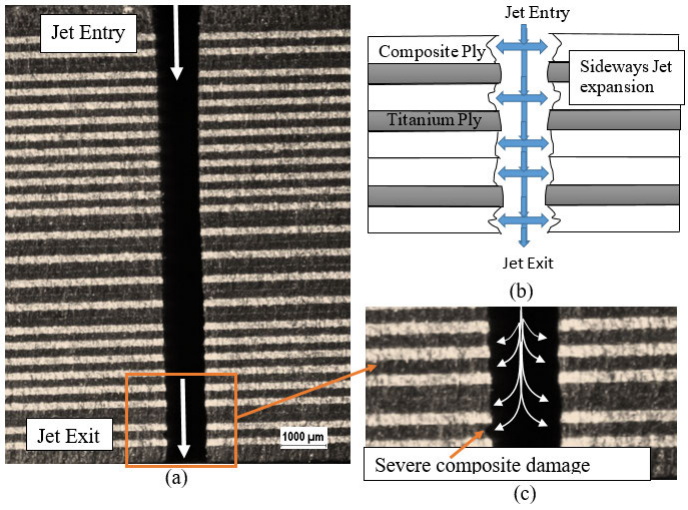

FIGURE 5. HYDRO-DISTORTION OF 10.5 mm THICK SPECIMEN MACHINED WITH AWJ-25 CONDITIONS DEPICTING (a) KERF WALL WITH JET PENETRATION DIRECTION, (b) GRAPHICAL ILLUSTRATION OF KERF DISTORTION, AND (c) JET EXIT KERF.

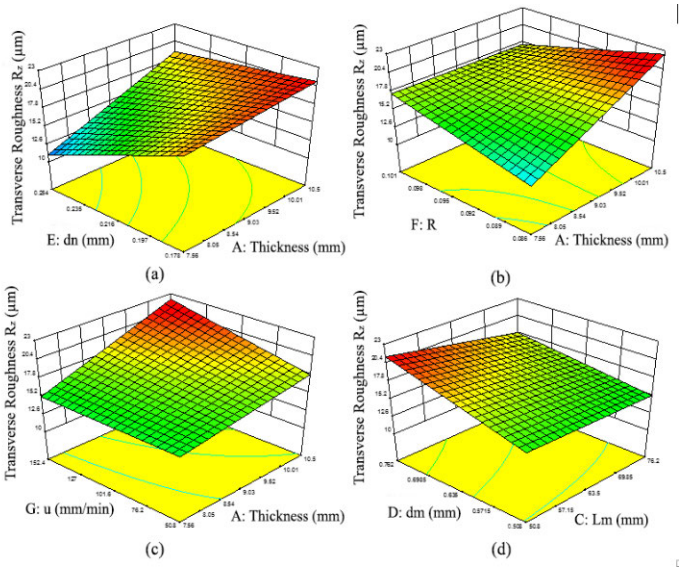

FIGURE 6. INTERACTION EFFECT BETWEEN (a) THICKNESS AND ORIFICE DIAMETER, (b) THICKNESS AND LOAD RATIO, (c) THICKNESS AND TRANSVERSE SPEED, (d) MIXING TUBE LENGTH AND DIAMETER ON TRANSVERSE ROUGHNESS R_z.

els. The effect clearly indicates an increase in jet exposure time and power transferred to the workpiece material at slower jet traverse speed, allowing a more efficient cut with decreased taper. Also, highest taper ratio was observed at largest orifice diameter (0.254mm) and highest traverse speed (152.4mm/min).

Surface Roughness

The irregularity of kerf wall is often related to jet curving due to loss of cutting energy near the exit side. This is generally characterized as rough cutting zone with undesirable striated pattern on machined composites [6,23,24] and metallic [21,25] surfaces. However, in fiber metal laminates, the kerf irregularity is not only contingent upon the machining conditions, but can also be attributed to significant difference in machinability of titanium and composite layers. One of the major limitations of AWJ machining of composites is the phenomenon of hydrowedging [13] where the water penetrates transverse to the jet flow direction and weakens the bonding between composite layers. A similar detrimental effect of water pressure build up was observed in Titanium-Graphite laminate where erosion of composite plies was found more than that of titanium plies. Figure 5 elucidates the kerf distortion phenomenon where jet expands sideways and erodes the composite matrix. The successive barrel-type kerf geometry observed in composite plies can be considered as a small notches, with radius up to 100 microns. Depending upon the service loading condition, these stress concentration sites may nucleate micro-cracks and prove highly detrimental to the structural strength. Upon visual inspection of high taper specimens, it was found that higher damage was near the entry and exit side where the composite ply concentration was high, and nearly square cut was observed where titanium was uniformly distributed. This can be attributed to the fact that titanium is removed by shearing, whereas composite plies involve fiber bending and series of fracture failure along with matrix bulk removal by the radial expansion of the jet. A TiGr laminate with titanium as face plies is expected to show less entry and exit damage. In order to quantitatively address the severity, transverse roughness parameter R_z was studied. Figure 6(a) shows the interaction effect of specimen thickness and orifice diameter. The maximum roughness observed was 21.1μm at small orifice bore size and for thicker specimen. The minimum roughness observed was 11.1μm at large orifice bore size and for thin specimen. The roughness was increased up to 72.4 ($\pm$1.4)% with reduction in orifice size and increment in specimen thickness. A small orifice diameter means less water mass flow rate, generating rougher surface. Also, higher thickness represents high penetration depth and more energy loss, leading to more erosive wear rather than sharp cutting at the exit side of the jet, generating a spiky, rougher surface.

As shown in Fig. 6(b), maximum roughness was observed at R=8.6% and for 10.5 mm thick specimen. A lower load ratio and increased jet penetration requirement reflect higher resistance in machining, justifying high R_z value. Figure 6(c) depicts the interaction effect between traverse speed and specimen thickness. As expected, a rougher surface was obtained at high jet traverse rate (u=152.4 mm/min) and for thicker specimen (10.5 mm) with

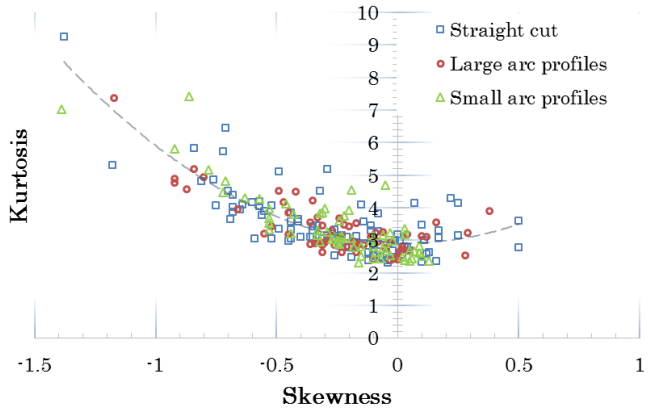

FIGURE 7. KURTOSIS AGAINST SKEWNESS PLOT FOR AWJ MACHINING PROCESS.

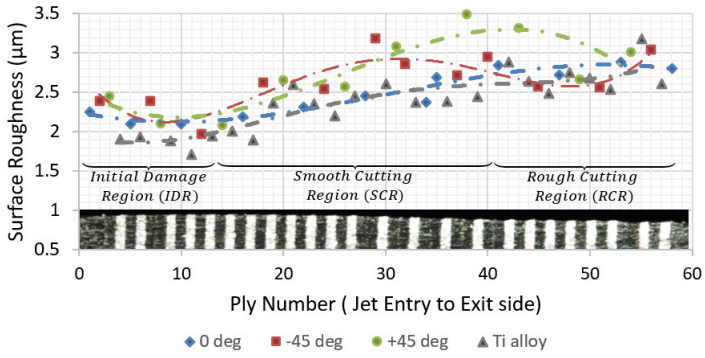

FIGURE 8. SURFACE ROUGHNESS (R_a) ALONG THE JET PENETRATION DIRECTION FOR EACH PLY IN STRAIGHT CUT FOR AWJ-32 SPECIMEN.

R_z=22.2μm. The effect of traverse rate was significant at higher thickness with 24.3% increase in roughness. Alternatively, the effect of thickness was significant at high traverse speed with 45.8% increase in roughness. Figure 6(d) depicts the interaction effect between mixing tube diameter and length. A rougher surface (R_z=21.3μm) was obtained with short mixing tube (50.8 mm) and large mixing tube diameter (0.762 mm). This indicates conditions of less coherent jet with reduced cutting efficiency. A high aspect ratio (Lm/dm=100 to 150) is desirable for low roughness with R_z between 15.3μm and 15.9μm.

Since AWJ process involves generation of new surfaces by the percussive action of stochastic abrasive particles, the surface topology studied with the third and fourth moment of profile distribution was useful in the process characterization. This is important to predict the functional behavior of the machined surface, such as fatigue and wear properties of mating surfaces. Figure 7 depicts the skewness (third moment) vs kurtosis (fourth moment) for AWJ machined transverse surfaces for TiGr laminate. The surface profiles were found to be negatively skewed and leptokurtic. The small arc profile kerfs showed least tendency for positive skewness when machined with Abrasive Waterjet. As evident from the taper results, the abrasive cutting component is distributed between components parallel and orthogonal to the jet traverse direction when traversing through a curved profile, which corresponds to the reduction in jet coherency. A negatively skewed profile indicates more resistance to abrasive erosion [14], which in this case is the reduced cutting efficiency of jet in the direction of jet penetration. Besides, the ratio of root mean square surface roughness and average surface roughness was to be around 1.28 ($\pm$0.025) which depicts the inherent characteristic of the machining process generated by random abrasive action.

Further, in order to investigate the surface roughness in the direction orthogonal to the jet penetration, 10.5 mm thick TiGr laminate, machined with experimental condition 32 (AWJ-32) was selected because a significant variation in surface roughness from top to bottom ply is expected for an AWJ profiled surface with conditions resulting in high taper. The average roughness (R_a) is plotted for each corresponding ply number, as shown in Fig. 8 with values ranging from 1.65μm to 3.5μm. Three zones can be identified based on the roughness values. The first zone - Initial Damage Region (IDR) spans around initial 8-9 plies ($\sim$1.2mm) with R_a value varying between 2.0-2.5μm for composite plies and 1.6-1.8μm for titanium plies. The value of R_a stabilizes and gradually increases up to the jet penetration depth of $\sim$8mm in SCR (Smooth Cuttng Region). The R_a value was observed between 2.25$-$3.5μm for composite plies and 2.2$-$2.45μm for titanium plies. The R_a value steeply increased in the remaining Rough Cutting Region (RCR) to up to 3.18μm. It was observed that the surface roughness of titanium plies was lower than the composite plies in all the cutting characterized regions, with an exception of the RCR where titanium depicted surface roughness nearly equivalent to the composite plies (>2.5μm). Besides, an unusual roughness characteristic was observed at the end of SCR where a discrete layup arrangement spans between ply number 27 and 42, with titanium plies interspersed alternatively between two consecutive composite plies instead of one. A sudden 8.5% drop in R_a value for titanium and 13% spurge for +45° composite ply suggests the effect of ply layup in machining laminates, significantly affecting the jet-material interaction. The effect of hydro-distortion becomes severe where composite percentage is high due to momentary hydro-pressure build up before each titanium ply, leading to smooth titanium surface on removal with high energy jet, and rougher composite surface due to increased water-induced distortion in composite plies. This is consistent with the observations made by Ramulu et al. [20]

Geometric Dependence

It was interesting to observe that the machining quality was significantly dependent on the cutting profile. The kerf taper ratio and transverse roughness (R_z) variation due to cutting geometry variation, when machined with a given set of AWJ process parameters, was as high as 20% and 61% respectively. The contribution of significant parameter terms in the machining responses - taper ratio and transverse roughness is depicted Fig. 9(a) and Fig. 9(b) respectively for five different cutting profile features. The contribution of mixing tube length was observed to increase with the cutting profile curvature in taper ratio model, while a negative trend was observed for mixing tube diameter. The orifice diameter contributed to less than 4% in taper ratio model. However, it shows maximum contribution to the transverse surface roughness of the kerf wall for nearly all curvatures. In comparison to straight cutting profile, the transverse roughness characteristics of large arcs were more sensitive to orifice diameter than mixing tube diameter, with 17.8−20% contribution in roughness model, and vice versa for small arced profiles with 6.5−17.5% contribution of mixing tube diameter in roughness model. It is clear that machining response is dependent on mixing tube and orifice diameter as far as cutting tool variables are concerned, and an optimum ratio of the bore sizes would be a reasonable objective for realizing a desired machining response for a given geometry.

Unlike transverse roughness response, pressure showed negligible contribution in taper ratio for all profile features. For transverse roughness, the contribution of pressure increased with the profile curvature. Also, the pressure contribution in transverse roughness is more for outer arc profiles than inner arcs. This involves the effect of jet dynamics and necessity for adequate control mechanism in contouring convex and concave profiles. The results also showed higher sensitivity of traverse speed for curved profiles in comparison to straight cuts. Besides, roughness was conspicuously affected by the thickness of the workpiece.

Mechanism of material removal was optically inspected for titanium, graphite fiber and thermoplastic matrix as different phases. Within the thermoplastic composite-titanium, matrix material is removed by shearing and plastic deformation as shown in Fig.10 and observed by Seo et al. [7] while carbon fibers were removed by micro chipping, brittle fracture, and bending failure [13]. Specimens with high abrasive flow rate showed signs of shear deformation on titanium ply concluding that titanium was removed by ductile shearing, abrasive plowing, and scratching action. Occasionally, dislodged titanium burrs were also found sticking over composite plies.

Parametric Optimization

The taper performance was found to be highly sensitive to geometrical variables. The selection of proper mixing tube and orifice is suggested as the first step in planning the waterjet machining of thick Titanium Graphite. Since the mixing tube length and diameter shows a variable trend with specimen thickness, the dimensions are required to be selected based on the same criteria. The orifice diameter is found to exhibit low taper at 0.178 mm ir-

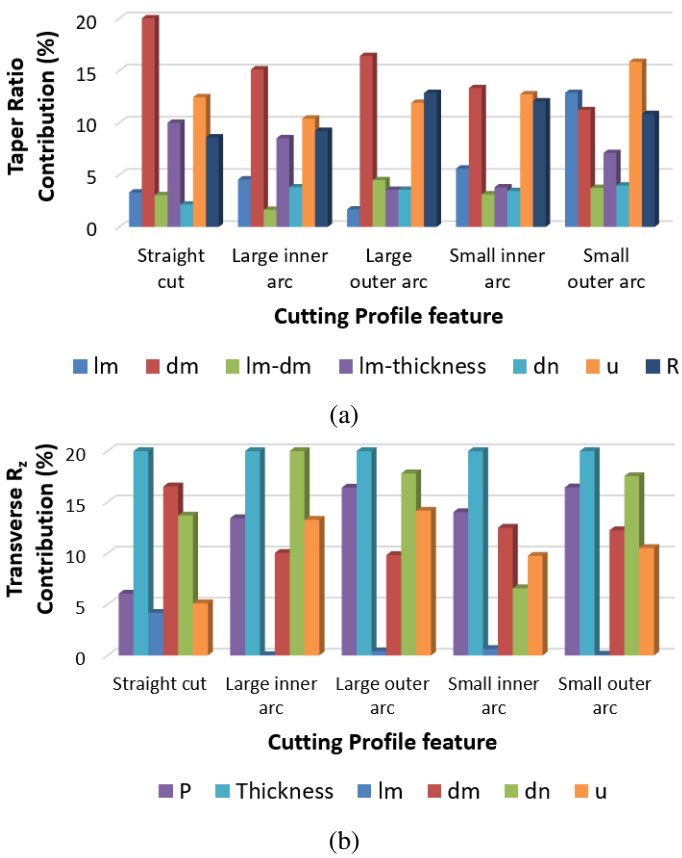

FIGURE 9. CONTRIBUTION (%) OF PROCESS PARAMETERS IN (a) TAPER RATIO MODEL, AND (b) TRANSVERSE ROUGHNESS R_z MODEL.

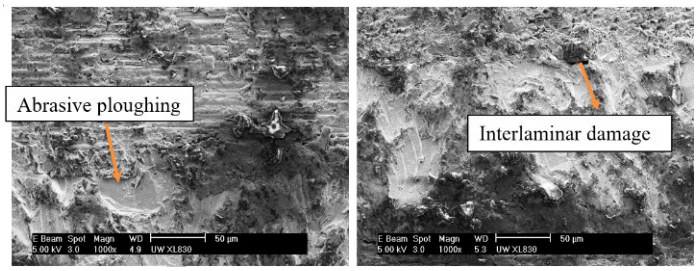

FIGURE 10. SEM MICROGRAPHS OF (a) FIFTH PLY FROM THE TOP, AND (b) EIGHTH PLY FROM THE BOTTOM OF 10.5 mm THICK, STRAIGHT CUT KERF WALL FOR AWJ-25 CONDITION.

respective of interaction with other parameters within the experimental limits. The water pressure is suggested to be minimum to account for the availability and reduced energy consumption. Besides, the process economics are significantly dependent on abrasive flow rate (or load ratio) and traverse speed, which are targeted to be low and high respectively for high material removal rate. The developed mathematical models were used to achieve a trade-off between conditions yielding low taper and low transverse R_z with a possible kerf roughness of $7.4-12.4\mu$m and taper ratio of $1.00-1.08$ for 7.56 TiGr laminate. However, optimized conditions achieved for 10.5 mm thick specimen showed higher roughness ($17.6-21.2\mu$m) and high taper ratio ($1.04-1.10$). The optimization results emphasize the disagreement within the conditions yielding high surface quality and low kerf taper for thick ($\sim$10.5mm) TiGr laminate. With the developed mathematical models, parametric optimization can be implemented for the desired objectives such as to minimize not only the machining quality, but also the contour severity due to geometric variance. The contour severity was successfully reduced with taper ratio and transverse R_z variation reduction to 5.6% and 20% respectively.

Comparison with Conventional milling

To foreground the merits of abrasive waterjet in machinability of TiGr, a comparative study was done between AWJ and conventional trimming. Figure 10(a,b) depicts a typical surface generated by AWJ. No signs of extensive damage or delamination were observed. However, when trimmed conventionally with same feed rate (152.4 mm/min), severe composite delamination and fiber pull outs were observed. Moreover, due to high temperature associated in conventional trimming process, the titanium was dislodged and smeared over the composite ply (Fig. 11(a,b)).

Figure 12 shows the SEM micrographs of conventionally trimmed surfaces (straight cut) at three different feed rates, two of them (50.8 and 152.4 mm/min) similar to jet traverse speed in AWJ. Titanium was removed by shearing, with evident machining marks at both 50.8 mm/min (Fig. 12(a)) and 152.4 mm/min (Fig. 12(b)) feed rate. At higher feed rate (635 mm/min), the titanium plies witnessed a decay of machining marks. However, scratch marks in the direction of feed suggest the plastic deformation and ductile fracture mode [26]. However, it was found that the damage to composite plies was the limiting factor to feed rate. At 152.4 mm/min feed rate the -45° plies showed significant batch pullouts, matrix distortion, damage and delamination. This trend was significantly accentuated at 635 mm/min feed rate as depicted in Fig. 12(c). On the contrary, Abrasive Waterjet showed rather more uniformly machined surface with less sensitivity to fiber orientation.

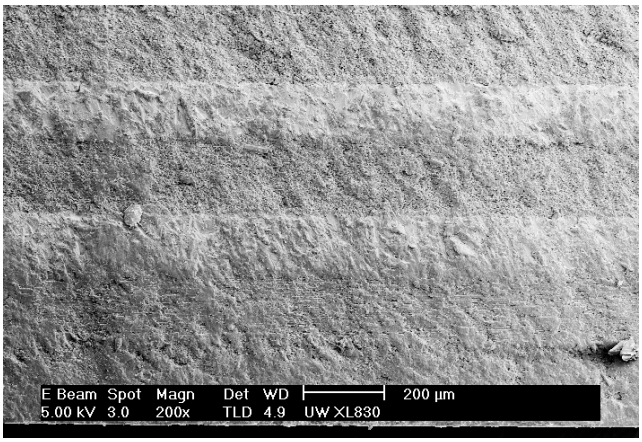

(a)

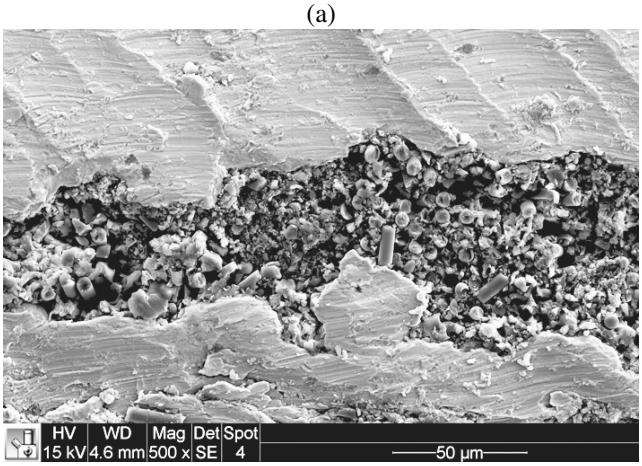

(b)

FIGURE 11. SEM MICROGRAPHS OF (a) AWJ MACHINED, AND (b) CONVENTIONALLY TRIMMED SURFACE AT 152.4 mm/min TOOL FEED RATE.

CONCLUSION

Abrasive Waterjet was successfully employed in contour machining of up to 10.5 mm thick TiGr FML. The machinability was investigated in terms of taper ratio and surface quality for different cutting profiles machined with conditions including seven controllable parameters. These parameters include pump pressure, jet traverse speed, load ratio (by varying abrasive flow rate), orifice diameter and mixing tube bore and length. SEM inspection revealed that the material removal mechanism was different for different material phases. Titanium was removed by shear deformation, scratching and abrasive ploughing. Within the composite material, matrix was removed by shearing, whereas graphite fibers were removed by micro chipping, brittle fracture, and bending failure. Small interply defects and dislodged titanium burrs were spotted over the composite ply. However the kerf surface was free from grit embedment. The

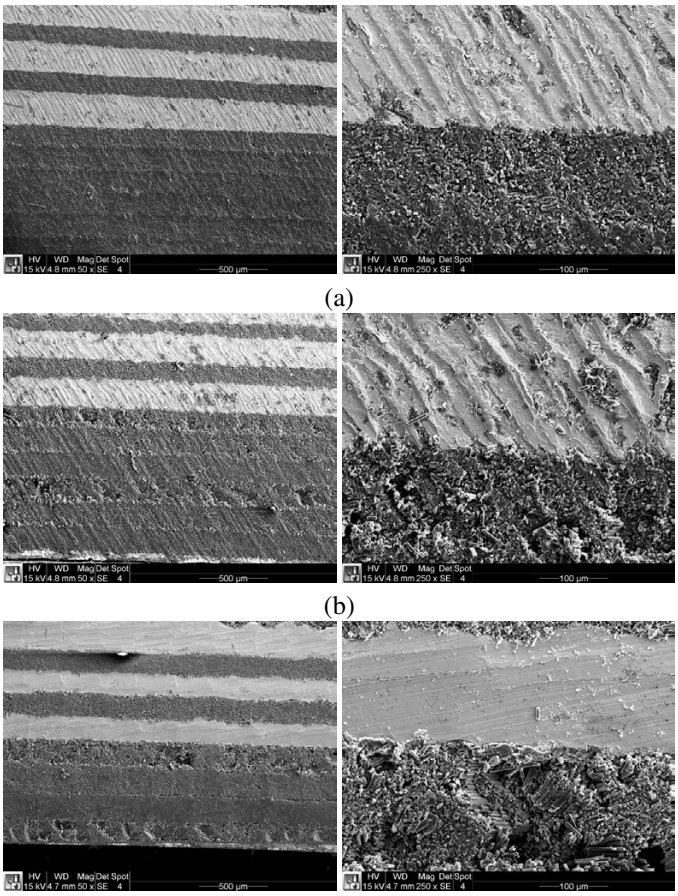

FIGURE 12. SEM MICROGRAPHS AT 50X AND 250X FOR CONVENTIONALLY MACHINED TiGr WITH (a) 50.8 mm/min, (b) 152.4 mm/min, AND (c) 635 mm/min TRAVERSE FEED RATE.

kerf wall topology was affected by the ply arrangement. Nearly square cuts (taper and water distortion free) can be achieved by avoiding continuous stacks of composite plies and maintaining laminates with higher percentage and uniform distribution of titanium plies. Low taper can be achieved by using Ultra High Pressure (600 MPa), low traverse speed (50.8 mm/min), high load ratio and high mixing tube to orifice bore ratio (0.23−0.33). An optimum mixing tube length to diameter ratio is necessary for desirable taper for a given thickness. Low Transverse kerf wall roughness ($R_z = 9.4\mu$m) can be achieved using lower pressure (380 MPa), low traverse speed (50.8 mm/min), high load ratio, high mixing tube to orifice bore ratio (0.5) and high mixing tube aspect ratio. The AWJ process was characterized in terms of R_q/R_a ratio and was determined to be 1.28 ($\pm$0.025). The process was negatively skewed and leptokurtic, similar to grinding process. The AWJ machining of thick TiGr specimens is conspicuously contingent upon the machining profile. The kerf taper ratio and transverse roughness variation when machined with a given process parameters was as high as 20 and 61% respectively. Parametric optimization (specifically, traverse speed and water pressure) can be used to reduce the contour severity of taper ratio and transverse R_z variation to 5.6% and 20% respectively. Besides, AWJ was found superior to conventional dry machining of TiGr. AWJ allows a greater processing window, low tool wear, less titanium burrs and low composite ply damage at higher feed rate.

ACKNOWLEDGMENT

The authors are thankful to Flow International for the supply of work material and technical support.

REFERENCES

[1] Burianek, D. A., and Spearing, S. M., 2002. "Fatigue damage in titanium-graphite hybrid laminates". *Composites Science and Technology,* ***62***(5), pp. 607–617.

[2] Ramulu, M., Stickler, P. B., McDevitt, N. S., Datar, I. P., Kim, D., and Jenkins, M. G., 2004. "Influence of processing methods on the tensile and flexure properties of high temperature composites". *Composites Science and Technology,* ***64***(12), pp. 1763–1772.

[3] Kim, D., and Ramulu, M., 2005. "Cutting and drilling characteristics of hybrid Titanium Composite Laminate (HTCL)". In Proceedings of 37th International SAMPE Technical Conference, Vol. 31, pp. 1–8.

[4] Abrate, S., and Walton, D. A., 1992. "Machining of composite materials. Part I: Traditional methods". *Composites Manufacturing,* ***3***(2), pp. 75–83.

[5] Arrazola, P.-J., Garay, A., Iriarte, L.-M., Armendia, M., Marya, S., and Le Maitre, F., 2009. "Machinability of titanium alloys (ti6al4v and ti555. 3)". *Journal of materials processing technology,* ***209***(5), pp. 2223–2230.

[6] Hashish, M., 1995. "Waterjet Machining of Advanced Composites". *Materials and Manufacturing Processes,* ***10***(6), pp. 1129–1152.

[7] Seo, Y., Ramulu, M., and Hashish, M., 2005. "Cost analysis of abrasive waterjet cutting: Thin sheet materials". In Proceedings of 37th International SAMPE Technical Conference, Vol. 37, pp. 1–12.

[8] Hamatani, G., and Ramulu, M., 1990. "Machinability of high temperature composites by abrasive waterjet". *Journal of Engineering Materials and Technology, Transactions of the ASME,* ***112***(4), pp. 381 – 386.

[9] Ramulu, M., and Arola, D., 1994. "The influence of abrasive waterjet cutting conditions on the surface quality of graphite/epoxy laminates". *International Journal of Machine Tools and Manufacture,* ***34***(3), pp. 295–313.

[10] Hashish, M., 1989. "Machining of advanced composites

with abrasive-waterjets". *Manufacturing Review,* ***2***(2), pp. 142–150.

[11] Shipway, P., Fowler, G., and Pashby, I., 2005. "Characteristics of the surface of a titanium alloy following milling with abrasive waterjets". *Wear,* ***258***(1), pp. 123–132.

[12] Seo, Y. W., Ramulu, M., and Kim, D., 2003. "Machinability of titanium alloy (Ti6Al4V) by abrasive waterjets". *Proceedings of the Institution of Mechanical Engineers, Part B: Journal of Engineering Manufacture,* ***217***(12), pp. 1709–1721.

[13] Ramulu, M., and Arola, D., 1993. "Water jet and abrasive water jet cutting of unidirectional graphite/epoxy composite". *Composites,* ***24***(4), pp. 299–308.

[14] Arola, D., and Ramulu, M., 1997. "Material removal in abrasive waterjet machining of metals Surface integrity and texture". *Wear,* ***210***(1-2), pp. 50–58.

[15] Azmir, M. A., and Ahsan, A. K., 2008. "Investigation on glass/epoxy composite surfaces machined by abrasive water jet machining". *Journal of Materials Processing Technology,* ***198***(1-3), pp. 122–128.

[16] Shanmugam, D. K., and Masood, S. H., 2009. "An investigation on kerf characteristics in abrasive waterjet cutting of layered composites". *Journal of Materials Processing Technology,* ***209***(8), pp. 3887–3893.

[17] Paul, S., Hoogstrate, A. M., and van Praag, R., 2002. "Abrasive water jet machining of glass fibre metal laminates". *Proceedings of the Institution of Mechanical Engineers, Part B: Journal of Engineering Manufacture,* ***216***(11), nov, pp. 1459–1469.

[18] Alberdi, A., Artaza, T., Suárez, A., Rivero, A., and Girot, F., 2015. "An experimental study on abrasive waterjet cutting of CFRP/Ti6Al4V stacks for drilling operations". *Int J Adv Manuf Technol.*, pp. 1–14. doi:10.1007/s00170-015-8192-x.

[19] Pahuja, R., Ramulu, M., and Hashish, M., 2014. "Abrasive Water jet machining (AWJ) of hybrid Titanium/Graphite composite laminate: Preliminary results". In BHR Group - 22nd International Conference on Water Jetting 2014, pp. 83 – 95.

[20] Ramulu, M., Isvilanonda, V., Pahuja, R., and Hashish, M., 2016. "Experimental investigation of abrasive waterjet machining of titanium graphite laminates". *International Journal of Automation Technology,* ***10***(3), pp. 392 – 400.

[21] Hashish, M., 1989. "A model for abrasive-waterjet (AWJ) machining". *Journal of Engineering Materials and Technology, Transactions of the ASME,* ***111***(2), pp. 154–162.

[22] Rozario Jegaraj, J. J., and Ramesh Babu, N., 2007. "A soft computing approach for controlling the quality of cut with abrasive waterjet cutting system experiencing orifice and focusing tube wear". *Journal of Materials Processing Technology,* ***185***, pp. 217–227.

[23] Arola, D., and Ramulu, M., 1996. "A study of Kerf characteristics in abrasive waterjet machining of graphite/ epoxy composite". *J. Eng. Mater. Technol.-Trans. ASME,* ***118***(2), pp. 256–265.

[24] Alberdi, A., Suárez, A., Artaza, T., Escobar-Palafox, G., and Ridgway, K., 2013. "Composite cutting with abrasive water jet". *Procedia Engineering,* ***63***, pp. 421–429.

[25] Raju, S. P., and Ramulu, M., 1994. "Predicting hydro-abrasive erosive wear during abrasive waterjet cutting: Part ii - an experimental study and model verification". *ASME, Production Engineering Division (Publication) PED,* ***68-1***, pp. 381 – 396.

[26] Yang, D., and Liu, Z., 2015. "Surface topography analysis and cutting parameters optimization for peripheral milling titanium alloy Ti-6Al-4V". *International Journal of Refractory Metals and Hard Materials,* ***51***, pp. 192–200.

Appendix A: Design of Experiments

TABLE 5. EXPERIMENTAL DESIGN

Experiment	Thickness	Pressure	Nozzle			Load Ratio	Traverse speed
	t (mm)	P (MPa)	dm (mm)	Lm (mm)	dn (mm)	R (%)	u (mm/min)
1	7.56	380	50.8	0.508	0.178	0.092	152.4
2	7.56	380	76.2	0.508	0.178	0.092	50.8
3	7.56	600	76.2	0.508	0.178	0.086	152.4
4	10.5	600	76.2	0.762	0.178	0.086	152.4
5	7.56	380	76.2	0.508	0.254	0.092	152.4
6	10.5	600	50.8	0.508	0.254	0.101	50.8
7	10.5	380	76.2	0.762	0.178	0.092	50.8
8	10.5	380	50.8	0.508	0.254	0.092	152.4
9	10.5	600	76.2	0.508	0.178	0.086	50.8
10	7.56	600	50.8	0.762	0.178	0.086	152.4
11	7.56	380	76.2	0.762	0.254	0.092	50.8
12	7.56	600	76.2	0.762	0.178	0.086	50.8
13	7.56	600	76.2	0.508	0.254	0.101	50.8
14	10.5	600	50.8	0.762	0.254	0.101	152.4
15	7.56	600	76.2	0.762	0.254	0.101	152.4
16	7.56	380	50.8	0.762	0.178	0.092	50.8
17	10.5	600	76.2	0.762	0.254	0.101	50.8
18	10.5	380	50.8	0.508	0.178	0.092	50.8
19	7.56	380	50.8	0.762	0.254	0.092	152.4
20	7.56	380	50.8	0.508	0.254	0.092	50.8
21	10.5	380	76.2	0.508	0.254	0.092	50.8
22	7.56	380	76.2	0.762	0.178	0.092	152.4
23	10.5	600	50.8	0.508	0.178	0.086	152.4
24	7.56	600	50.8	0.508	0.178	0.086	50.8
25	10.5	380	50.8	0.762	0.178	0.092	152.4
26	10.5	380	76.2	0.508	0.178	0.092	152.4
27	7.56	600	50.8	0.762	0.254	0.101	50.8
28	10.5	380	50.8	0.762	0.254	0.092	50.8
29	7.56	600	50.8	0.508	0.254	0.101	152.4
30	10.5	380	76.2	0.762	0.254	0.092	152.4
31	10.5	600	50.8	0.762	0.178	0.086	50.8
32	10.5	600	76.2	0.508	0.254	0.101	152.4